Experimental Verification of Bremsstrahlung Production and Dosimetry Predictions as a Function of Energy and Angle

D. E. Beutler, J. A. Halbleib, T. W. L. Sanford, and D. P. Knott

Abstract—**Measurements of energy deposition from bremsstrahlung production as a function of angle and beam energy (5–25 MeV) are shown to be in excellent agreement with Monte Carlo predictions. Dosimetry measurements are made and predicted in both equilibrated and underequilibrated radiation environments. In the latter case the quality of the agreement requires an accurate prediction of both the photon and electron spectra produced by the primary electron beam. An improved empirical equation for predicting bremsstrahlung production is also presented. This empirical relation can be used to estimate doses without resorting to expensive calculational efforts. It also gives an analytical relationship for dose as a function of energy and angle for a converter optimized for bremsstrahlung production using 15.5 MeV electrons.**

I. Introduction

THE integrated TIGER series (ITS) of coupled electron/photon Monte Carlo transport codes [1]–[3] is widely used to predict the radiation output from flash x-ray sources and for the design of bremsstrahlung converters [4]. The codes are also used to predict the response of radiation diagnostics (e.g., thermoluminescent dosimeters (TLD's)) and the response of electronic components and subsystems. Hence, the demonstration of the validity of the ITS codes for these applications is important.

Flash x-ray sources themselves are not the most suitable instruments for code verification because of the relatively poorly defined phase space distribution of the source electrons that is available as input for the Monte Carlo calculation. Earlier work using a Pelletron accelerator has shown that the ITS codes provide an excellent description of the radiation environment produced by low-energy electrons [5]–[9]. In addition, we have recently demonstrated the ability of the codes to predict TLD doses for the radiation environment produced by monoenergetic electrons at a single energy (15.5 MeV) for a variety of bremsstrahlung converter designs where Compton and pair-production processes dominate [10], [11]. However, no direct experimental verification had been made of the ability of the codes to predict spectra and/or TLD doses as a function of both energy and angle in this high-energy regime. Nor has a verification of ITS predictions of dose attenuation with depth as a function of attenuation material for high-energy bremsstrahlung been performed.

Accordingly, we carried out a set of measurements on the EG&G electron linac [12] at Santa Barbara, CA, using TLD dosimeters to address this deficiency. We have made a detailed absolute comparison of these measurements with simulations using the ACCEPT code of the ITS system. Each Monte Carlo simulation included both the production of the radiation by the electron beam interacting with a bremsstrahlung target and the subsequent interaction of that radiation with the TLD's and their surroundings [11], [13].

These measurements and comparisons to calculations serve a fourfold purpose. They 1) verify the operation of the ITS codes in this energy regime, 2) characterize the bremsstrahlung fields and the subsequent TLD dosimetry responses typical of pulsed sources used to simulate the effects of intense bursts of γ-rays, 3) demonstrate the voltage and angular dependence of the dose and dose-area product for use in flash x-ray design and analysis, and 4) provide a more complete database for benchmarking other radiation transport codes. We also have used these data to evaluate and improve the empirical Martin equation [14]–[16], which is often used to estimate radiation dose from optimized bremsstrahlung converters.

This paper only addresses the energy and angular dependence of high-energy bremsstrahlung. A separate publication addresses the comparison of measured dose attenuation as a function of depth of on-axis bremsstrahlung with ITS predictions [17].

In the next section we present our experimental details. The third section discusses details of the code simulations followed by a fourth section on the empirical equations developed to estimate radiation dose. In the fifth section we compare our measured data to both code simulations and empirical equations, and in the last section we summarize our conclusions.

Manuscript received May 10, 1994; revised August 10, 1994. This work was supported by the U.S. Department of Energy under Contract DE-AC04-94AL85000.

D. E. Beutler, J. A. Halbleib and T. W. L. Sanford are with the Sandia National Laboratories, Albuquerque, NM 87185.

D. P. Knott is with the Technical Support Corporation, Albuquerque, NM 87185.

IEEE Log Number 9405594.

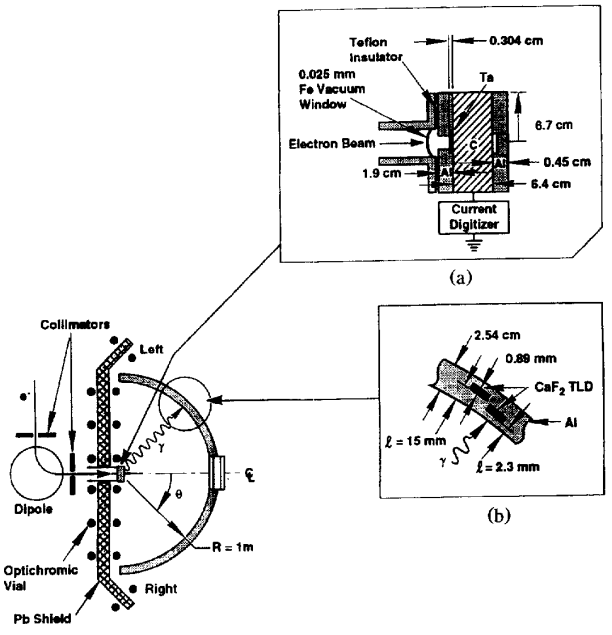

Fig. 1. Diagram of the experimental setup. (a) Details of bremsstrahlung target. (b) Details of the arc dosimetry fixture.

II. Experimental Details

A. EG&G Linac

The EG&G linac was used to generate a well-defined and controllable electron beam (Fig. 1). The linac produces an ~ 1-cm diameter, 20-ns-wide electron pulse at a bremsstrahlung converter. The spread in electron energy was 3% with a 0.5% absolute uncertainty in the mean over the range of energies used. At the beginning and end of each exposure a thin phosphor screen was inserted at 45° relative to the beam upstream of the converter in the vacuum line to verify the diameter and centering of the electron beam. The phosphor was in the beam for less than 1% of the radiation time and we found no evidence in previous work [11] that this perturbed the irradiation in any way.

The beam was extracted through a 25-μm stainless steel window and impinged on the downstream converter at normal incidence (Fig. 1(a)). The converter consists of 3.04 mm of tantalum, 6.40 cm of carbon ($\rho = 1.75$ g/cm^3), and 4.5 mm of aluminum. The dimensions and materials were chosen to match an optimized converter for 15.5-MeV electrons. This arrangement is identical to that used in previous work [10], [11]. Five different electron beam energies were used in this study: 5.5, 10.6, 15.5, 20.5, and 25.1 MeV. The charge deposited in the converter was measured with a current integrator so that an absolute comparison of the measured dose per unit charge deposited (Gy(CaF_2)/C) with the ITS predictions could be made. The linac was shielded with lead upstream of the converter to prevent electrons and photons scattered from the machine and energy analyzing equipment from contributing to the measured bremsstrahlung output. The scattered radiation was monitored with optichromic dosimeters [18] placed before and after the lead shielding. These were read immediately following each irradiation to check for contamination of our primary dosimetry measurements. An additional source of scattered radiation is a concrete wall located ~ 2 m downstream from the converter, probably the major source of scattered radiation in our measurements. Measurements of dose using the optichromic dosimeters and TLD measurements with the electron beam blocked yield values ~ 50 Gy(CaF_2)/C. This background scattered radiation can skew the magnitude of the dosimetry measurements of the bremsstrahlung when their values become comparable. Fortunately, this skewing was only found at large angles at the lowest electron beam energies.

B. Dosimetry Fixture

The fixture used to examine the photon/electron radiation field shall be referred to as the arc and is described in more detail in [10] and [11]. It provides dose measurements at two depths l, as well as measuring the angular dependence of the field as a function of half angle θ (Fig. 1). Square CaF_2:Mn TLD's (3.17 × 3.17 × 0.89 mm) were used to measure the absorbed dose with an uncertainty of ~ 7% and were read by the Sandia Radiation Dosimetry Laboratory [19].

The arc (Fig. 1(b)) is an aluminum (6061 ASTM alloy) semicircle 2 m in diameter. TLD's are distributed at ~ 1° intervals and are surrounded by two different thicknesses of aluminum. The TLD's in the inner semicircle have 0.62 g/cm^2 of aluminum in front (l = 2.3 mm) and 5.69 g/cm^2 behind, while the TLD's in the outer arc have 4.05 g/cm^2 of aluminum in front (l = 15 mm) and 2.26 g/cm^2 behind. Other work has shown [10], [11], [17] that 1 g/cm^2 of aluminum in front and 0.2 g/cm^2 behind is sufficient to provide electron equilibration in the TLD for 5.5 MeV bremsstrahlung, and 5 g/cm^2 of aluminum in front and 1g/cm^2 behind is sufficient at 25.1 MeV. Hence, all the TLD's have adequate equilibration at all energies from the back, and for the outer arc all but the highest energy (25.1 MeV) have adequate equilibration in front. The arc was placed with the converter at its center so that all the TLD's were approximately 1 m from the radiation source. The TLD's behind the thicker aluminum are designed to give the angular dependence of the dose primarily from the photon spectrum, whereas those behind the thinner aluminum are also sensitive to the electrons emitted from the target at the higher energies [10], [20]. With this fixture we measure the angular distribution of the radiation field in the forward hemisphere over an angular range of ±90°.

III. Code Simulations

The primary motivation for this work was the experimental verification of a model [11] that is employed extensively in the design and analysis of high-intensity flash x-ray sources for the simulation of nuclear radiation effects. These high-power sources are not suitable for benchmarking the model due to the difficulty in defining

the electron distributions incident upon the bremsstrahlung target and their relatively poor shot-to-shot reproducibility. Indeed, the model, along with diagnostics measurements, is often used to infer or corroborate these distributions. The model consists of a modification of the ACCEPT code, Version 2.1, of the ITS system, which simulates the production and transport of the radiation cascade in three-dimensional geometries. The primary modification to the Monte Carlo model is a variation on the full-transport (FT) algorithm described in the appendix of [14]. The FT algorithm is a highly coupled set of variance reduction procedures that make possible the practical simulation of combined radiation-production/radiation-response applications. The advantage of using this algorithm is that it avoids the necessity for carrying out a pair of decoupled calculations, one for radiation production and one for radiation response, with their attendant inaccuracies. These inaccuracies result from the loss of information when the entire energy and angle distribution of the radiation production calculation is not used as input to the response calculation and by neglecting any possible interaction, for example, radiation backscattering, of the source and deposition regions. The FT capability has been developed over the past several years and is being continuously refined. It should be emphasized that there is no modification of the cross sections themselves or the way they are used in the Monte Carlo calculations; hence comparisons with the experiment discussed here represent a bona fide test of the existing physical model of the ITS system. Electron energies were sampled from a flat spectrum over the narrow range of $\pm 1.5\%$ of the incident electron energy. The electrons were normally incident on the converter configuration of Fig. 1(a) and were sampled from a uniform beam of radius 0.375 cm. Measurement of the deposited normalizing beam charge excluded electrons stopping in the stainless steel entrance window or supporting flange of exiting the target, whereas the Monte Carlo outputs were normalized to the charge in the incident beam. A correction factor, equal to the ratio of the deposited to incident charge, was obtained from the Monte Carlo simulations and applied to the predictions. These correction factors, from highest to lowest electron beam energy, are 0.94, 0.94, 0.93, 0.91, and 0.86.

Run times for each simulation were approximately 1.5 to 3 hours on an IBM RISC/6000, model 560. With these times, we were able to keep most statistical uncertainties under 5%.

IV. Martin Equation

Because predictions of the bremsstrahlung production are elaborate and require large amounts of computer resources, an empirical formula is often desirable for predicting flash x-ray machine output. The traditional equation, often referred to as the Martin equation [14]–[16], is

$$\frac{D}{Q} = (1.7 \times 10^3) V^{2.65} e^{-\theta V/2.1} \tag{1}$$

where D is the exposure (measured in roentgens) at an angle θ (measured in radians) at a distance 1 m downstream of the target, Q is the incident charge measured in coulombs, and V is the kinetic energy of the incident electrons measured in MeV. This equation predicts the exposure per unit charge assuming a fluence-optimized converter for each energy. Previous work has shown that this equation, although in excellent agreement with measured data for angles $< 15°$ [21], is not applicable for predictions of dose at larger angles [11]. This limitation is not surprising, because large-angle data was not available when (1) was generated [22].

We have formulated a new empirical equation using the thick equilibrator data obtained in this study. We chose the thick equilibrator data because these data best approximate an equilibrium dose in the TLD's and reflect dose obtained from the photon environment. Our aim is to preserve the functional form of (1) as much as possible because of its accuracy at small angles, yet extend the validity of its angular range. Hence, we refer to our new empirical equation as the modified Martin equation:

$$\frac{D}{Q} = (3.14) V^{3.18} e^{-(0.616(\theta V)^{0.641}} \tag{2}$$

where the variables and units are the same as in (1), except that D is now in units of dose ($Gy(CaF_2)$) and Q is the charge *deposited* in the converter in coulombs. The additional coefficient (0.641) in the exponent is primarily responsible for extending the range of angles for good agreement with our experimental data from 15° to 90°.

Summarizing, there are three major differences in how these equations are formulated in addition to the added coefficient in the exponent. The Martin equation is expressed in terms of exposure and the incident electron charge and assumes an optimized converter for each electron energy. The modified Martin equation is expressed in equilibrium dose TLD and charge deposited in the bremsstrahlung converter, and uses a converter optimized for 15.5-MeV electrons. The difference between incident and absorbed charge is small ($< 15\%$). However, the converter design assumption does have a major impact on the expected dose (exposure) and should be considered when comparing the two equations. This is especially true for the lower electron energies (< 10 MeV) where the converter used is far from optimum in thickness. At higher electron energies the doses are not a strong function of the converter thickness [4].

The coefficients for the modified Martin equation were obtained by performing a least-squares fit of the data for each energy over all angles to determine the two coefficients in the exponent. The overall uncertainty in these coefficients was 7%. The other two coefficients were determined by fitting the 0° data as a function of voltage. The overall uncertainty in the latter coefficients was 1%. Because we gave equal weighting to the errors in fitting the data, the larger magnitude data at small angles dominate the value of the fitted parameters. We show that in

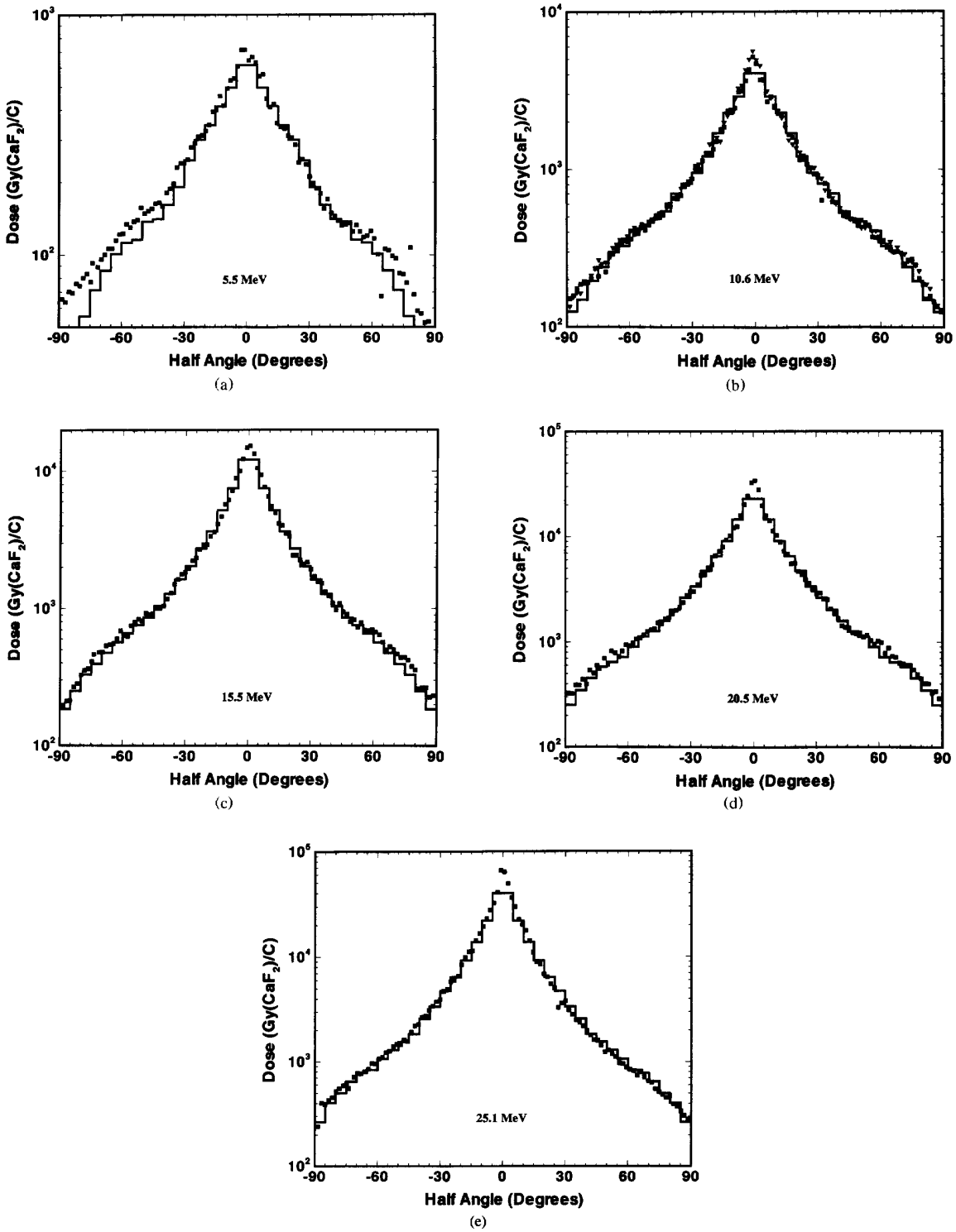

Fig. 2. Plot of measured and ITS-predicted dose per unit deposited charge as a function of half angle θ for the 15-mm (thick) aluminum front buffer for various primary electrons. (a) 5.5 MeV. (b) 10.6 MeV. (c) 15.5 MeV. (d) 20.5 MeV. (e) 25.1 MeV. The filled squares and triangles represent measured data and the histograms are the code predictions.

TABLE I
COMPARISON OF MEASURED, PREDICTED, AND MODIFIED MARTIN DOSE-AREA PRODUCTS

Incident Energy (MeV)	Half Angle (Degrees)	Front Aluminum Thickness (mm)	Measured Dose-Area (Gy-m^2/C)	ITS-Predicted Dose-Area (Gy-m^2/C)	Ratio (ITS/Measured)	Modified Martin Dose-Area (Gy-m^2/C)	Ratio (Mod. Martin/Measured)
5.5	30	15.0	306	290	0.948	253	0.827
5.5	30	2.3	327	297	0.908	---	---
5.5	60	15.0	653	619	0.948	599	0.917
5.5	60	2.3	748	648	0.866	---	---
5.5	90	15.0	924	830	0.898	860	0.931
5.5	90	2.3	1070	886	0.828	---	---
10.6	30	15.0	1404	1370	0.976	1313	0.935
10.6	30	2.3	1334	1408	1.055	---	---
10.6	60	15.0	2598	2639	1.016	2553	0.983
10.6	60	2.3	2770	2797	1.010	---	---
10.6	90	15.0	3347	3343	0.999	3234	0.966
10.6	90	2.3	3727	3634	0.975	---	---
15.5	30	15.0	3269	3229	0.988	3127	0.957
15.5	30	2.3	3235	3147	0.973	---	---
15.5	60	15.0	5585	5574	0.998	5310	0.951
15.5	60	2.3	6205	5967	0.962	---	---
15.5	90	15.0	6870	6742	0.981	6237	0.908
15.5	90	2.3	7851	7424	0.946	---	---
20.5	30	15.0	5790	5727	0.989	5651	0.976
20.5	30	2.3	5248	5270	1.004	---	---
20.5	60	15.0	9277	9293	1.002	8628	0.930
20.5	60	2.3	9610	9481	0.987	---	---
20.5	90	15.0	11080	10887	0.983	9629	0.869
20.5	90	2.3	11965	11478	0.959	---	---
25.1	30	15.0	8753	8470	0.968	8439	0.964
25.1	60	15.0	12858	12815	0.997	11930	0.928
25.1	90	15.0	14668	14639	0.998	12891	0.879

most cases the agreement at large angles is still good for this improved equation.

V. COMPARISONS

A. Code Predictions Versus Measurements

Because we used the full transport modification of the ITS code, calculations can be used to predict the dose in both thickly buffered (l = 15 mm) and thinly buffered (l = 2.3 mm) TLD's. In all the figures shown in this section, we plot dose per unit deposited charge as a function of angle for the primary electron beam energies used.

For the thickly buffered TLD data and ITS predictions shown in Fig. 2, the aluminum buffering should be sufficient to prevent energy deposition from any external electrons and produce an equilibrium dose from the incident photons in the TLD's for all but the 25.1-MeV energy. Only at this energy is the aluminum slightly thinner than the minimum front thickness for an equilibrium dose (15 mm as compared to 18.6 mm for equilibrium [17]). Hence, these measurements should be dominated by the photon response. The agreement here is excellent for all energies, except for large angles at the 5.5-MeV energy (Fig. 2(a)), where the data becomes comparable to our background level of $\sim$ 50 Gy(CaF_2)/C. For Fig. 2(b), two sets of measured data at the 10.6-MeV energy (filled squares and triangles), taken 6 months apart with different accelerator shielding, are plotted. These data agree to within the measurement errors and give us confidence that our measurement technique is stable and that the data are reproducible.

Another useful measure of agreement between measurements and predictions in the comparison of dose-area product. We define the dose-area product to be

$$DA(\theta) = 2\pi R^2 \int_0^{\theta} D(\Theta) \sin \Theta \, d\Theta \tag{3}$$

where DA is the dose area product taken on the surface of a sphere as a function of half angle θ, $D(\Theta)$ is the dose at a particular angle assuming circumferential symmetry about the normal (see Fig. 1), and R is the radius of the arc. For the measured data, we averaged the TLD data at corresponding negative and positive angles, and assumed this dose was constant up to half the angular spacing of the TLD's on either side. The dosimetry predictions are symmetric by design and constant over each angular bin. Comparisons of dose-area product between measurements and predictions are given in Table I. Predicted dose-area products agree with measurements, which use

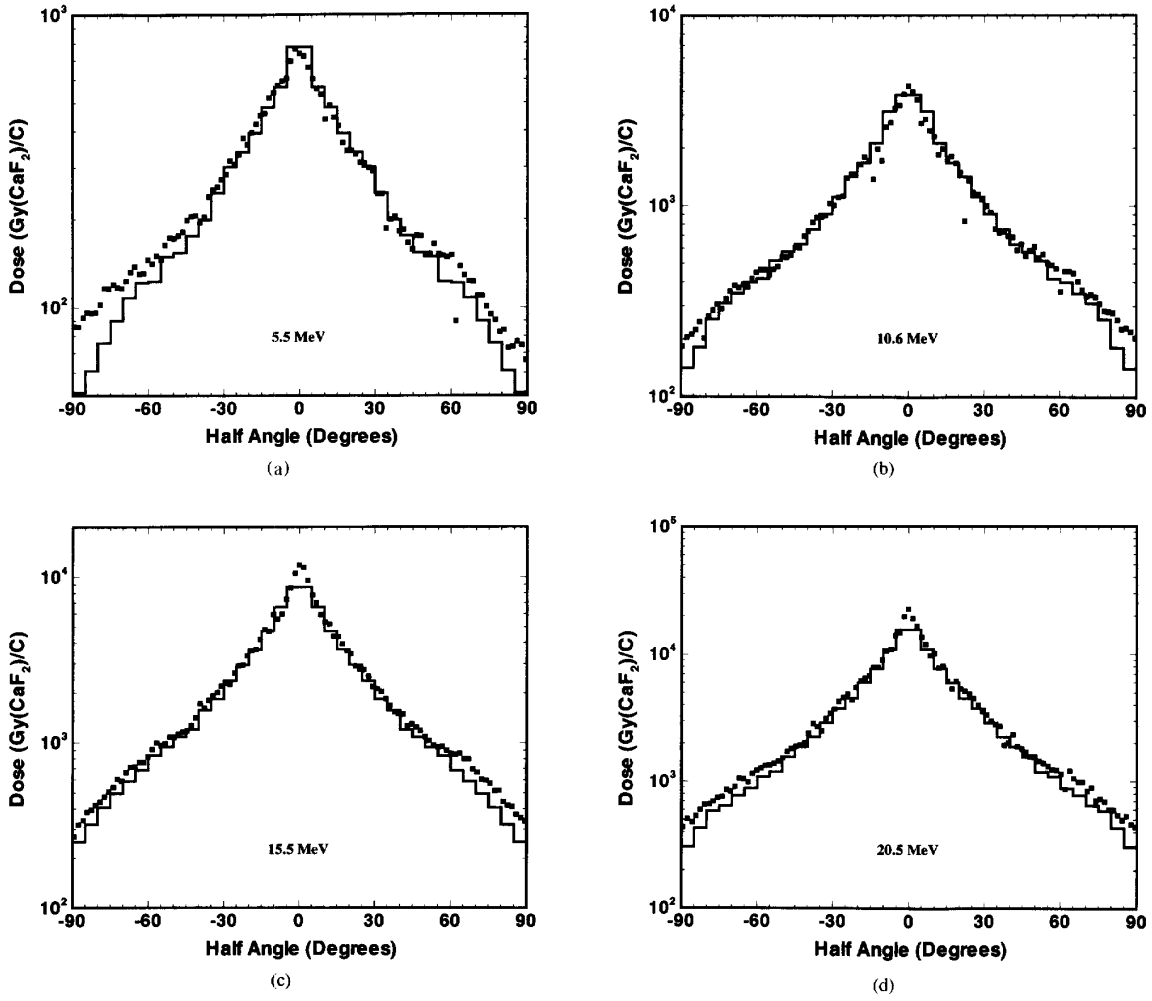

Fig. 3. Plot of measured and ITS-predicted dose per unit deposited charge as a function of half angle θ for the 2.3-mm (thin) aluminum front buffer for various primary electrons. (a) 5.5 MeV. (b) 10.6 MeV. (c) 15.5 MeV. (d) 20.5 MeV. The filled squares represent measured data and the histograms are the code predictions.

the thick front aluminum thickness, for all angles and energies within 5% for all energies except for the 5.5-MeV, 90° dose-area product, where the difference is 10%, again due to the background radiation.

Predicting the dose is nonequilibrated TLD's is a more stressful test of ITS because it requires accurate predictions of both the photon and electron spectra emanating from the converter. In Fig. 3 we plot the thinly buffered TLD data and ITS predictions. No data was taken using the thinly buffered TLD's at the 25.1-MeV energy because the thickly buffered TLD's were also potentially "thin" at this energy and the number of TLD's available was limited. There is more disagreement at large angles than was seen in Fig. 2. This may still be due to contamination of the measurements by scattered radiation from sources not included in the model used in the ITS calculations. This is more apparent at large angles where the doses are lower. It is to be expected that the more thinly buffered TLD's would be more sensitive to an electron or soft photon scattered radiation environment. In addition, the ~ 50 Gy(CaF_2)/C background value for the scattered radiation only applies to radiation produced without the electron beam incident on the converter. It does not include the scattered radiation produced from the desired photon and electrons emanating from the converter and interacting with the shielding and room walls. This source of energy deposition is also not included in the ITS predictions. Despite this discrepancy, the agreement is still good and gives us confidence that the ITS code can accurately predict both the electron and photon spectra. Comparisons of predictions and measurements of dose-area product for the nonequilibrated case are given in Table I. Predicted dose-area products agree with measurements, which use the thin front aluminum thickness,

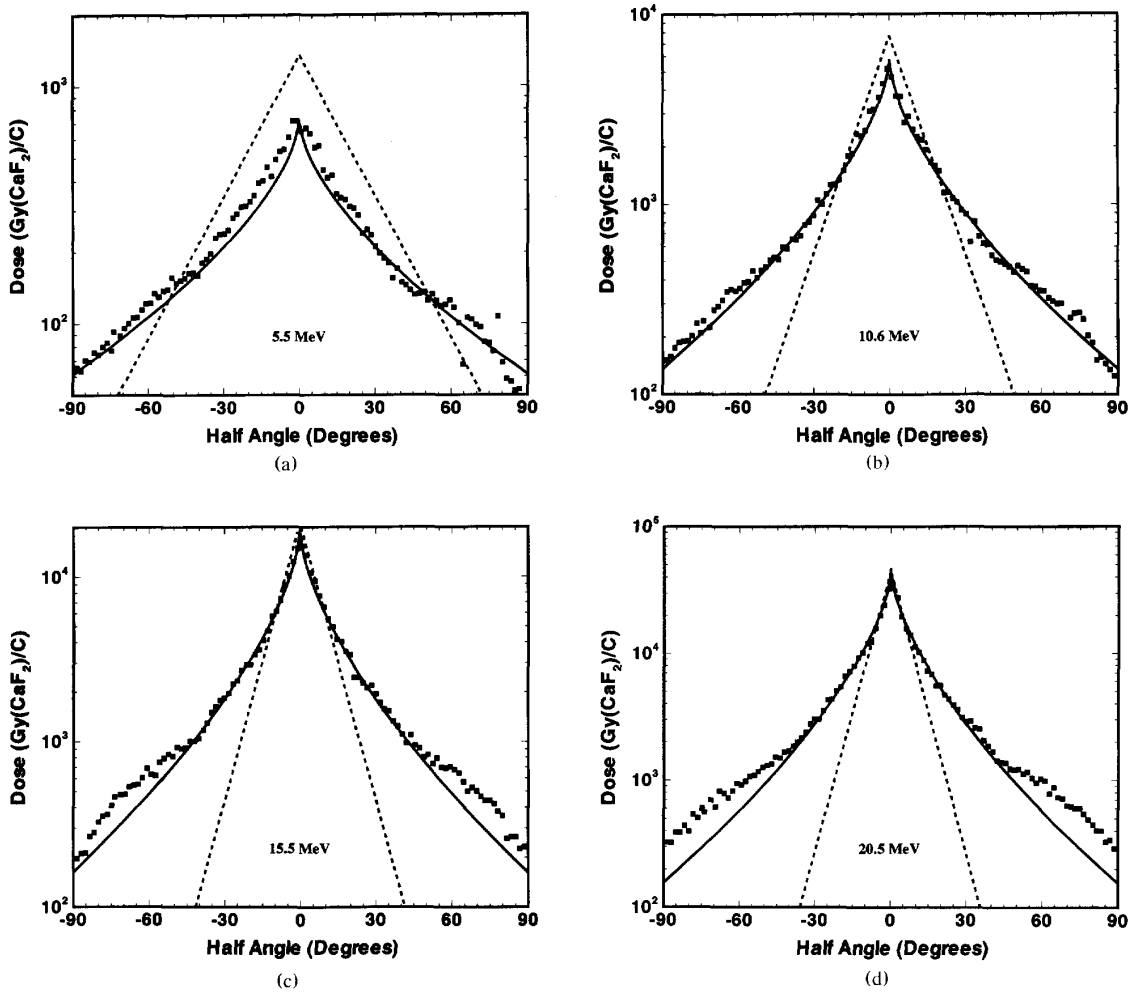

Fig. 4. Plot of measured (filled squares), Martin predicted (dashed line), and modified Martin predicted (solid line) dose per unit deposited charge as a function of half angle θ, using 15-mm aluminum front buffer for various primary electrons. (a) 5.5 MeV. (b) 10.6 MeV. (c) 15.5 MeV. (d) 20.5 MeV. The filled squares represent measured data, the dashed line represents the Martin equation, and the solid line represents the modified Martin equation.

for all angles and energies within 5% for all energies except for the 5.5-MeV dose-area products, where the differences range from 9 to 17%.

For both buffer thicknesses, the agreement between measurements and ITS predictions is better than had been observed previously at the 15.5 MeV energy [10], [11], particularly in the region between 15° and 30°. This is due to corrections of small errors in the converter geometry description used in the previous model predictions. Otherwise, the earlier measurements and calculations applied are equivalent to those performed here at 15.5 MeV.

B. Empirical Equations Versus Measurements

In Figs. 4 and 5, we plot the measured dose per unit deposited charge using the thickly buffered (l = 15 mm) TLD's as a function of angle for the five different energies. These data are the same as those plotted in Fig. 2. In addition, values obtained from the Martin and the modified Martin equations are shown.

The Martin equation underpredicts the measured dose per unit measured charge at large angles for all energies and overpredicts the small angle dose for the 5.5-MeV and 10.6-MeV cases. This latter disagreement can be attributed to the converter not being optimized for these low energies, as is assumed by the Martin equation. However, the large-angle disagreement makes the Martin equation unsuitable for predicting dose or dose-area products where large solid angles are involved.

The modified Martin equation is in better agreement with the data. This is to be expected, because the coefficients were obtained by fitting the functional form of (2) to this data set. It does show, however, that the functional form of (2) is appropriate to describe the energy deposition from the bremsstrahlung production. Comparisons of

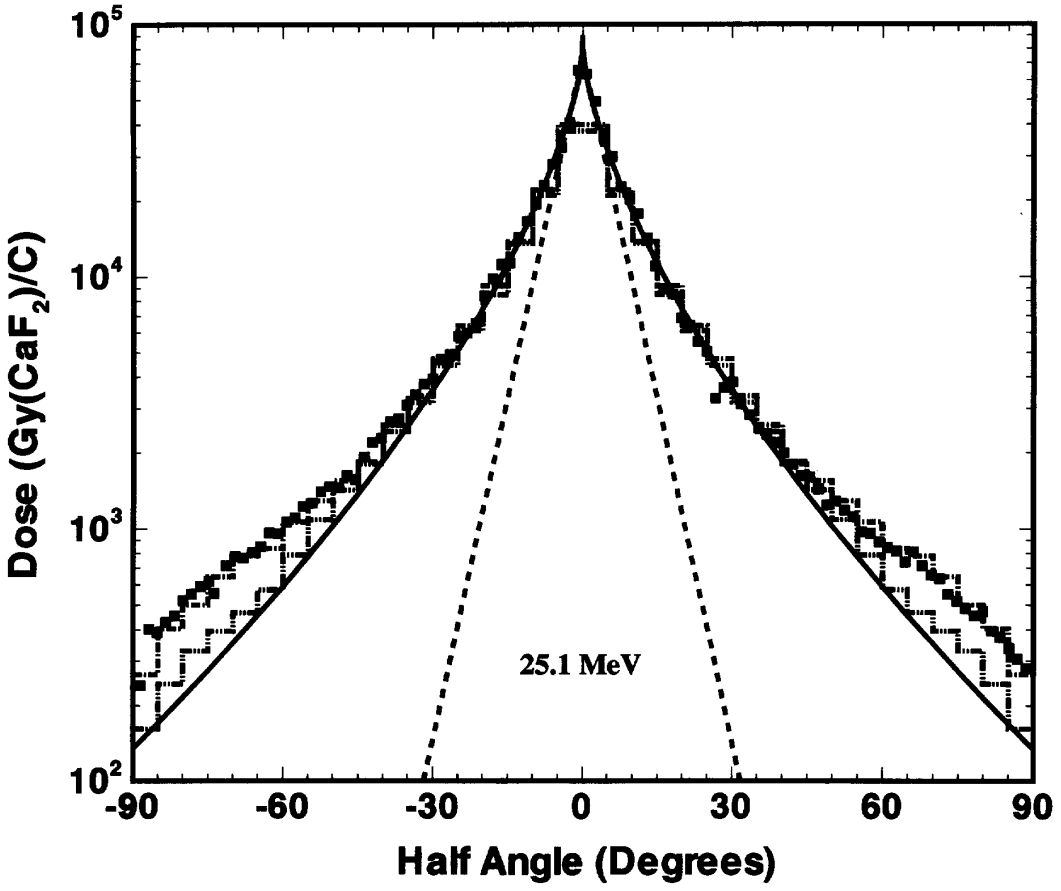

Fig. 5. Plot of measured (filled squares), Martin predicted (dashed line), and modified Martin predicted (solid line) dose per unit deposited charge as a function of half angle θ using the 15-mm aluminum front buffer for 25.1-MeV primary electrons. The filled squares represent measured data, the dashed line represents the Martin equation, and the solid line represents the modified Martin equation. The "dot-dash" histogram represents the ITS prediction and the "dot-dot-dash" histogram represents the ITS calculation using a converter 3 times larger in diameter.

dose-area product between measurements and modified Martin predictions are given in Table I. Predicted dose-area products agree with measurements, which use the thick front aluminum thickness, for all angles and energies within 17%. Thus, the modified Martin equation (2) is an improvement over the standard Martin equation (1) when large angles need to be considered and a converter optimized for 15.5 MeV is used. It also can be an inexpensive alternative to computer intensive calculations for dose predictions in this parameter range and the functional form given in (2) is a useful model for fitting similar data of this type.

We did notice a systematic deviation of the modified Martin predictions at high energies and large angles (Figs. 4(c) and (d) and Fig. 5). Because the dose at large angles is small relative to the on-axis dose, especially at the higher energies, it has little impact on the fitting parameters obtained by minimizing the sum of the square of the absolute errors. We hypothesize that these differences between the modified Martin predictions and the data may be due to the sides of the converter becoming thin to the high energy radiation. This would cause an increase in the measured radiation at large angles and high electron energies over the modified Martin predictions. To examine this possibility, we performed an additional ITS calculation at the 25.1-MeV electron energy using a converter 3 times larger in diameter to approximate the response of a truly 1-D converter. This result is plotted in Fig. 5 along with the original ITS prediction shown in Fig. 2(e). The original ITS prediction is in good agreement with the measured data. The quasi-1-D ITS prediction is in much better agreement with the modified Martin predictions. This suggests that the modified Martin equation may be more relevant and may be in better agreement for bremsstrahlung converters that closely approximate a 1-D structure.

As a final comparison of measurements, ITS predictions, and modified Martin equation, we fit each of these

TABLE II
COMPARISON OF FITTING PARAMETERS TO (4) USING MEASURED, PREDICTED, AND MODIFIED MARTIN DOSE-AREA PRODUCTS

Half angle	Measured		Modified Martin		ITS Predicted	
(Degrees)	*a*	*b*	*a*	*b*	*a*	*b*
5	0.175	2.71	0.136	2.77	0.296	2.50
10	0.743	2.56	0.697	2.57	1.54	2.30
15	1.94	2.42	1.86	2.42	3.76	2.18
20	3.94	2.29	3.76	2.29	6.81	2.09
25	6.76	2.18	6.44	2.19	10.5	2.09
30	10.8	2.08	9.93	2.09	14.6	1.97
40	18.0	1.97	19.1	1.95	24.0	1.88
50	27.9	1.88	30.4	1.84	34.9	1.80
60	40.3	1.79	43.0	1.75	47.5	1.73
70	53.7	1.72	55.7	1.68	59.3	1.68
80	65.3	1.68	76.0	1.59	68.9	1.65
90	72.7	1.65	78.6	1.59	75.5	1.63

to a simple function for a number of half angles θ (see Fig. 1). This function can be expressed as

$$DA = aV^b \tag{4}$$

where DA is the dose-area product in (Gy-m^2/C), V is the incident electron voltage in MeV, and a and b are empirical fitting parameters. These fitting parameters obtained from the measurements and predictions are shown in Table II. The uncertainty in the mean of these parameters is $< 5\%$. The agreement between the different sets is good. One can also use this information to determine the dependence of the dose on incident electron energy in this energy range. For on-axis radiation the dose is a very strong function of energy ($b \sim 2.7$), which is in good agreement with the standard Martin equation (1). However, over the entire forward hemisphere the energy dependence is much weaker ($b \sim 1.6$). Hence, our work illustrates, as was also shown in [23], that the strong dependence of on-axis dose is due in large part to the forward peaking of the radiation and is not simply the increase in efficiency of bremsstrahlung production with electron energy.

VI. CONCLUSIONS

We have measured the energy deposition from bremsstrahlung production for all forward angles and over the range of primary electron energies from 5.5 to 25.1 MeV. Using this data, we have verified the ability of the ITS code to predict energy deposition from bremsstrahlung production over this range of angles and energies. This agreement of data and predictions has been demonstrated for geometries where the photon and the combined photon/electron radiation environments are important. In addition, we have developed an improved Martin equation, which can be used in lieu of expensive calculations to aid designers and experimenters at high-energy flash x-ray facilities in estimating the radiation output of machines as a function of energy and angle. Although the coefficients for this equation were derived using our measured data obtained using a single converter thickness, this converter thickness is reasonably close to optimum for incident electron energies > 10 MeV and < 30 MeV. In addition, because we have verified the ability of the ITS to predict energy deposition in this range, one can easily use this code to generate coefficients for other empirical equations based on other converter designs using the form of the modified Martin equation without the need for further measurements.

REFERENCES

[1] J. A. Halbleib and T. A. Mehlhorn, "ITS: The integrated TIGER series of coupled electron/photon Monte Carlo transport codes," Sandia National Laboratories Report No. SAND84-0573, Nov. 1984.

[2] J. A. Halbleib and T. A. Mehlhorn, "ITS: The integrated TIGER series of coupled electron/photon Monte Carlo transport codes," *Nucl. Sci. Eng.*, vol. 92, no. 2, pp. 338, 1986.

[3] J. A. Halbleib, "Structure and operation of the ITS code system" and "Applications of the ITS codes," in *Monte Carlo Transport of Electrons and Photons*, T. M. Jenkins, W. R. Nelson, and A. Rindi, (Eds.). Plenum Publishing Corp., 1988, pp. 249–284.

[4] T. W. L. Sanford and J. A. Halbleib, "Radiation output and dose predictions for flash x-ray sources," *IEEE Trans. Nucl. Sci.*, vol. NS-31, no. 6, pp. 1095–1100, 1984.

[5] G. L. Lockwood, L. E. Ruggles, G. H. Miller, and J. A. Halbleib, "Calorimetric measurement of electron energy deposition in extended media—Theory versus experiment," Sandia National Laboratories Report SAND79-0414, Jan. 1980.

[6] G. J. Lockwood, L. E. Ruggles, G. H. Miller and J. A. Halbleib, "Electron energy and charge albedos—Calorimetric measurement versus Monte Carlo theory," Sandia National Laboratories Report SAND80-1968, Nov. 1981.

[7] T. W. L. Sanford, J. A. Halbleib, and W. Beezhold, "Experimental check of bremsstrahlung dosimetry predictions for 0.75-MeV electrons," *IEEE Trans. Nucl. Sci.*, vol. NS-32, no. 6, pp. 4410–4415, 1985.

[8] T. W. L. Sanford, J. A. Halbleib, W. Beezhold, and L. J. Lorence, Jr., "Experimental verification of non equilibrated bremsstrahlung dosimetry predictions for 0.75 MeV electrons," *IEEE Trans. Nucl.Sci.*, vol. NS-33, no. 6, pp. 1261–1265, 1986.

[9] D. E. Beutler, J. A. Halbleib, and D. P. Knott, "Comparison of experimental pulse height distributions on germanium detectors with integrated Tiger series code predictions," *IEEE Trans. Nucl. Sci.*, vol. NS-36, no. 6, pp. 1912–1919, 1989.

[10] D. E. Beutler, J. A. Halbleib, T. W. L. Sanford, D. P. Knott, and D. L. Fehl, "Dosimetry considerations for the high-energy photon/electron environment of HERMES III: Implications for experiments and modeling," *IEEE Trans. Nucl. Sci.*, vol. NS-38, no. 6, pp. 1736–1745, 1991.

[11] T. W. L. Sanford, D. E. Beutler, J. A. Halbleib, and D. P. Knott,

"Experimental verification of bremsstrahlung production and dosimetry predictions for 15.5 MeV electrons," *IEEE Trans. Nucl. Sci.*, vol. NS-38, no. 6, pp. 1160–1170, 1991.

[12] N. J. Norris, J. L. Detch, S. M. Kocimskl. C. R. Sawyor, and C. L. Hudson, "EG & G electron linac modifications," in *Proc. 1986 Linac Accelerator Conference*, Stanford, CA, 1986, pp. 546.

[13] J. A. Halbleib and J. R. Lee, "Predicted radiation environment of the Saturn baseline diode," Sandia National Laboratories Report SAND87-1650, Sept. 1987, p. 73 (appendix).

[14] HWH/JCM/82/8, "Re-evaluation of the bremsstrahlung production efficiency for optimum targets," Atomic Weapons Research Establishment, England, Internal Memo.

[15] T. H. Martin, "Determination of bremsstrahlung production efficiencies from data obtained on Phermex at 27 MeV," Sandia National Laboratory Report SC-DR-69-240, May, 1969.

[16] ——, "A computerized method of predicting electron beam bremsstrahlung radiation with specific application to high voltage flash x-ray machines," Sandia National Laboratories Report SC-RR-69-241, May, 1969.

[17] T. L. W. Sanford, J. A. Halbleib, D. E. Beutler, and D. P. Knott, "Experimental verification of dosimetry predictions of bremsstrahlung attenuation as a function of material and electron energy," *IEEE Trans. Nucl. Sci.*, vol. NS-40, no. 6, pp. 1409–1417, 1993.

[18] R. R. Radak and W. L. McLaughlan, "The gamma-ray response of optichromic dosimeters," *Radiat. Phys. Chem.*, vol. 23, no. 6, pp. 673–675, 1984.

[19] L. M. Choate, T. R. Schmidt, G. A. Zawadzkas, (Eds.) "Sandia National Laboratories Radiation Facilities," Sandia National Laboratory Report SAND89-1399, Dec. 1989.

[20] F. H. Attix, *Introduction to Radiological Physics and Radiation Dosimetry*. New York: Wiley, 1986.

[21] T. W. L. Sanford, P. D. Coleman, and J. W. Poukey, "Measurement and interpretation of electron angle at MABE beam stop," Sandia National Laboratories Report SAND84-1423, Feb. 1986 (see Figs. 18 and 19).

[22] J. C. Martin, private communication with T. W. L. Sanford.

[23] T. W. L. Sanford, J. A. Halbleib, J. W. Poukey, C. E. Heath, and R. Mock, "Dose-voltage dependence of coaxial bremsstrahlung diodes," *Nucl. Instr. Meth. Phys. Res.*, vol. B34, pp. 347–356, 1988.